Formulation of liposomes functionalized with the Lotus lectin and effective in targeting highly proliferative cells

Formulation of liposomes functionalized with *Lotus* lectin and effective in targeting highly proliferative cells

Cinzia Della Giovampaola, Antonietta Capone, Leonardo Ermini, Pietro Lupetti, Elisa Vannuccini, Federica Finetti, Sandra Donnini, Marina Ziche, Agnese Magnani, Gemma Leone, Claudio Rossi, Floriana Rosati, Claudia Bonechi

PII: S0304-4165(17)30015-6
DOI: doi:10.1016/j.bbagen.2017.01.015
Reference: BBAGEN 28741

To appear in: *BBA - General Subjects*

Received date: 16 September 2016
Revised date: 21 December 2016
Accepted date: 13 January 2017

Please cite this article as: Cinzia Della Giovampaola, Antonietta Capone, Leonardo Ermini, Pietro Lupetti, Elisa Vannuccini, Federica Finetti, Sandra Donnini, Marina Ziche, Agnese Magnani, Gemma Leone, Claudio Rossi, Floriana Rosati, Claudia Bonechi, Formulation of liposomes functionalized with *Lotus* lectin and effective in targeting highly proliferative cells, *BBA - General Subjects* (2017), doi:10.1016/j.bbagen.2017.01.015

Formulation of liposomes functionalized with *Lotus* lectin and effective in targeting highly proliferative cells

Cinzia Della Giovampaola,[1] Antonietta Capone,[1] Leonardo Ermini,[1,2] Pietro Lupetti,[1] Elisa Vannuccini,[1] Federica Finetti,[1] Sandra Donnini,[1] Marina Ziche,[1] Agnese Magnani,[3,5] Gemma Leone,[3,5] Claudio Rossi,[3,4] Floriana Rosati[1] and Claudia Bonechi[3,4*]

[1]Department of Life Sciences, University of Siena, Via Aldo Moro 2, 53100 Siena, Italy

[2]Program in Physiology & Experimental Biology, Hospital for Sick Children, Toronto, Canada

[3]Department of Biotechnology, Chemistry, and Pharmacy, University of Siena, Via Aldo Moro 2, 53100 Siena, Italy

[4]CSGI, Research Center for Colloids and Nanoscience, University of Florence, Via della Lastruccia 3, 50019 Sesto Fiorentino (FI)

[5]INSTM, Research Center for Materials Sciences and Technologies, Via G. Giusti 9, 50121 Firenze

Keywords: targeted liposomes/lotus lectin/doxorubicin/drug delivery/NMR

**Corresponding authors:*

Dr. Claudia Bonechi

Dept. Biotechnology, Chemistry and Pharmacy, University of Siena

Via Aldo Moro 2

53100 Siena, Italy

phone +39 0577 234372

fax +39 0577 234254

claudia.bonechi@unisi.it

Abbreviations

Doxorubicin (Dox)

Lectin from *Lotus tetragonolobus* (LTL)

1,2-dioleoyl-*sn*-glycero-3-phosphocholine (DOPC)

1,2-di-(9Z-octadecenoyl)-sn-glycero-3-phosphoethanolamine (DOPE)

DOPC/DOPE (1:1) liposomes (L)

FITC-dextran (Dex)

Lotus lectin-functionalized-liposomes (LTL-L)

Lotus lectin-functionalized-FITC-dextran-encapsulated-liposomes (LTL-Dex-L)

FITC-dextran-encapsulated-liposomes (Dex-L)

Dox-encapsulated-liposomes (Dox-L)

Lotus lectin-functionalized-Dox-encapsulated-liposomes (LTL-Dox-L)

ABSTRACT

Background. Liposomes, used to improve the therapeutic index of new and established drugs, have advanced with the insertion of active targeting. The lectin from *Lotus tetragonolobus* (LTL), which binds glycans containing alpha-1,2-linked fucose, reveals surface regionalized glycoepitopes in highly proliferative cells not detectable in normally growing cells. In contrast, other lectins localize the corresponding glycoepitopes all over the cell surface. LTL also proved able to penetrate the cells by an unconventional uptake mechanism.

Methods. We used confocal laser microscopy to detect and localize *LTL*-positive glycoepitopes and lectin uptake in two cancer cell lines. We then constructed doxorubicin-loaded liposomes functionalized with LTL. Intracellular delivery of the drug was determined *in vitro* and *in vivo* by confocal and electron microscopy.

Results. We confirmed the specific localization of *Lotus* binding sites and the lectin uptake mechanism in the two cell lines and determined that LTL-functionalized liposomes loaded with doxorubicin greatly increased intracellular delivery of the drug, compared to unmodified doxorubicin-loaded liposomes. The LTL-Dox-L mechanism of entry and drug delivery was different to that of Dox-L and other liposomal preparations. LTL-Dox-L entered the cells one by one in tiny tubules that never fused with lysosomes. LTL-Dox-L injected in mice with melanoma specifically delivered loaded Dox to the cytoplasm of tumor cells.

Conclusions. Liposome functionalization with LTL promises to broaden the therapeutic potential of liposomal doxorubicin treatment, decreasing non-specific toxicity.

General Significance. Doxorubicin-LTL functionalized liposomes promise to be useful in the development of new cancer chemotherapy protocols.

INTRODUCTION

Liposomes are artificially constructed phospholipid vesicles with an aqueous inner volume; they have been explored for drug delivery in cancer therapy [1]. Compared to non-encapsulated chemotherapeutic drugs, liposomes have several advantages: they accumulate preferentially at cancer sites; they have lower clearance than free drugs; they can be loaded with multiple anticancer drugs and chemotherapeutics; they improve solubility of hydrophobic drugs, reduce the potential immunogenicity of drugs [2] and can be designed to exert maximum activity at the intracellular pH of tumors [3]. The side effects associated with conventional drug delivery can also be reduced. An excellent example is the significant reduction in irreversible toxicity of free doxorubicin when transported by liposomes [4,5].

Drug delivery systems have recently been decked with biorecognitive ligands having affinity for receptors at the desired site of action. The immune system with its specific antibody-antigen interaction has provided most recognition molecules [6] and now glycobiology with its interactions between carbohydrate- and sugar-binding proteins called lectins, has begun to contribute to biorecognition delivery strategy [7]. In cancer there is increasing evidence of the role of glycosylation in tumor formation and metastasis [8]. Alterations in cell surface glycosylation, particularly terminal motifs, such as fucosylation [9] and sialylation or branching and truncation of N-and O-chains, appear to be common themes among cancer-associated changes in glycan structures [10]. As the significance of glycan changes increases, the search for specific glycan-based drug targets is widely pursued. The lectin from *Ulex europaeus* has been found to specifically bind colon carcinoma tissues but not normal cells; thus Rh-I-UEA-1 liposomes that selectively target adenomatous polyps in APCMin/+ mice have been constructed [11]. Liposomes coated with the lectin from *Wheat germ* (WGA) are reported to efficiently target intestinal cells for drug delivery [12] and lectin grafted nanocarriers have also been used for gene delivery [13].

We recently demonstrated that when used at high concentrations, the lectin from *Lotus tetragonolobus* (LTL), which preferentially binds glycans with alpha-1,2-linked fucose, reveals surface glycoepitopes in highly proliferative cells not detectable in cells with normal growth rate [14]. The epitopes were found in restricted regions close to the nucleus. The lectin proved able to penetrate the cells by an unconventional uptake mechanism [14]. Another fucose-binding lectin, which prefers glycans with alpha-1,6-linked fucose and localized glycans all over the cell surface, was taken up by a conventional mechanism [14]. Binding and uptake mechanisms were demonstrated in venule endothelial cells (CVEC) [14].

In the present study we confirmed the presence and restricted location of LTL-positive surface molecules and the unconventional LTL uptake mechanism in human cancer cell line DU145 and murine cancer cell line B16-F10. We then used LTL to construct liposomes that could target these

cancer cells. Vesicles with 1,2-dioleoyl-sn-glycerophosphocholine (DOPC) and 1,2-dioleoyl-sn-glycerophosphoethanolamine (DOPE) were thus formed. DOPC and DOPE are commonly used in zwitterionic liposomes, since they form a fluid bilayer at room temperature and since phosphocholine and phosphoethanolamine are the most abundant polar head types in the outer cell membrane [15]. Zwitterionic liposomes are chemically stable, easily synthesized and without strong toxicity toward mouse fibroblast and astrocyte cell cultures [16]. We functionalized the liposomes with LTL and compared their efficiency and modality in penetrating cells of cancer cell lines DU145 and B16-F10 with the efficiency and modality of non functionalized liposomes, by following the fluorescence of encapsulated dextran or doxorubicin or by analyzing the cells by electron microscopy. Their efficacy in reaching tumor cells after systemic *in vivo* administration was also investigated.

MATERIAL AND METHODS

Chemicals

Doxorubicin (99% purity, Dox), dextran conjugated to fluorescein (99% purity, Dex) and solvents were purchased from Sigma Aldrich (St. Louis, MO, USA). Lectin (99% purity, LTL) and biotin-conjugated lectins were purchased from Vector Laboratories (Burlingame, CA, USA). DOPC (1,2-dioleoyl-*sn*-glycero-3-phosphocholine; >99% purity) and DOPE (1,2-di-(9Z-octadecenoyl)-sn-glycero-3-phosphoethanolamine) were purchased from Avanti Polar Lipids Inc. (Alabaster, AL, USA).

Cell cultures

Human prostate cancer cell line DU145 and murine melanoma cancer cell line B16-F10 were plated in 10 cm diameter dishes in EMEM (Eagle Minimum Essential Medium) supplemented with 10% fetal bovine serum (FBS) (Hyclone, Logan, UT, USA). Media were used after addition of 2 mM l-glutamine and antibiotics (100 U/ml penicillin and 100 U/ml streptomycin). The cell lines were obtained from American Type Culture Collection (ATCC, Rockville, MD, USA). All reagents were purchased from Sigma Aldrich (St. Louis, MO, USA).

Binding and uptake of lectins

1.0-2.0 × 10^4 cells/well were seeded on glass cover-slips into 24-multiwell plates, cultured for 24 h in appropriate medium, then, for binding experiments, first fixed with 4% paraformaldehyde (PFA), extensively washed and finally incubated in the lectins. For uptake experiments, the cells were first incubated for different time intervals with lectins and then fixed with 4% PFA. For binding and uptake analyses, the following biotin-conjugated lectins were used: 2.5 μg/ml ConA (*Canavalia ensiformis* agglutinin), 25 μg/ml LTL (*Lotus tetragonolobus* lectin), 2.5 μg/ml AAL (*Aleuria aurantia* lectin). The lectins were suspended in PBS for binding and in culture medium for uptake. Biotin-conjugated lectins were detected with Alexa Fluor 488-conjugated streptavidin (Invitrogen, Thermo Fisher Scientific, Eugene, OR, USA). Uptake inhibition of the lectins was tested by incubating the cells, 30 min before and 30 min after addition of lectins, with 80 μM Dynasore (Sigma Aldrich, St. Louis, MO, USA) in 0.2% DMSO or 0.2% DMSO only (vehicle control) in EMEM. At the end of all fluorescence experiments, the cover slips were mounted in Fluormount (Sigma Aldrich, St. Louis, MO, USA) and visualized with a LSM 700 confocal laser scanning microscope (Zeiss, Jena, Germany). The images were processed in *LSM Image* (Zeiss, Jena, Germany) or Adobe Photoshop 7.0 (Adobe Systems, Mountain View, CA, USA).

Background due to endogenous biotin or biotinylated proteins was eliminated using a *Streptavidin/Biotin Blocking Kit* (Vector Laboratories, Burlingame, CA, USA). After blocking and

prior to addition of biotinylated lectins, the cells were pre-treated with the kit streptavidin solution for 90 min, rinsed briefly with PBS and then incubated for 90 min with the biotin solution.

Western blot analysis

Cells were incubated with the biotin-conjugated lectins for 3 hours, washed with DPBS (Dulbecco's Phosphate Buffered Saline, Lonza, Verviers, Belgium) and then detached with 0.25% Trypsin-EDTA solution (Sigma Aldrich, St. Louis, MO, USA) at 37°C. The detached cells were washed in DPBS, centrifuged at 500 × g for 10 min and the pellet solubilized in Sample Buffer [17]. Lysates of 2.0×10^5 cells were separated by 10% sodium dodecyl sulfate polyacrylamide gel electrophoresis (SDS-PAGE), transferred to a nitrocellulose membrane and probed with peroxidase (POD)-conjugated streptavidin (Sigma Aldrich, St. Louis, MO, USA). Reactivity was detected by *ImmunoStar TM HRP Chemiluminescent Kit* (BioRad Microscience, MA, USA) and observed by Chemi-Doc XRS (BioRad Microscience, MA, USA) gel imaging system. Densitometric analysis of the reactive bands was conducted with *Quantity One* software (BioRad Microscience, MA, USA).

Preparation of lectin-oleic acid conjugate

200 μL oleic acid (Sigma Aldrich; MW:282.47; δ=0.891 g/mL) was added to 10.0 mL absolute ethanol to obtain $6.3x10^{-4}$ M solution. Subsequently, N-hydroxysuccinimide (NHS, $6.3x10^{-3}$ M), N3-(dimethylaminopropyl)-N′-ethylcarbodiimide hydrochloride (EDC, $6.3x10^{-3}$ M) and lectin ($6.3x10^{-4}$ M) were added and maintained at 4°C overnight. After 24 hours, 50 mL bi-distilled water was added to remove excess NHS and EDC and to recover the lectin-oleic acid conjugate. FTIR spectra of native oleic acid and lectin-oleic acid complex were recorded using a Nicolet Thermo 5700 spectrometer equipped with an attenuated total reflection (ATR) accessory with a 45° end-face germanium crystal as internal reflection element (IRE). The spectra were acquired between 4000 and 750 cm^{-1} at a resolution of 2.0 cm^{-1} by a procedure already reported [18] (Table 1S and Figure 1S).

Liposome preparation

The liposomal formulation consisted of DOPC and DOPE at 1:1 molar ratio, with a total lipid concentration of $1.0x10^{-2}$ M. Liposomes were prepared in a round-bottom vial by mixing appropriate amounts of stock solutions selected among DOPC, DOPE, lectin-oleic acid conjugate, FITC-Dextran and doxorubicin, on the basis of formulation design. Liposomes were synthetized with the following molar ratios: LTL-L (1:250); Dex-L (0.4:250); LTL-Dex-L (1:0.4:250); LTL-Dox-L (1:50:250); Dox-L (50:250). A dry lipid film (with or without doxorubicin) was obtained by

evaporating the solvent under vacuum overnight. Rehydration with Milli-Q grade H_2O (or D_2O for NMR experiments) yielded multilamellar dispersion. Multilamellar vesicles were obtained by vortexing and were then subjected to eight freeze/thaw cycles in liquid nitrogen and water bath at 40°C. This method improved size distribution homogeneity of the final suspension. Liposomes were subsequently reduced in size and converted to unilamellar vesicles (LUVs) by extrusion through 100 nm or 50 nm polycarbonate membranes. Twenty-seven passages were performed with the LiposoFast apparatus (Avestin, Ottawa, Canada). LUVs were stored at room temperature. The residual non-encapsulated doxorubicin was removed by dialysis.

Size and surface charge of liposomes

The size and surface charges of loaded and non-loaded functionalized liposomes were measured by dynamic light scattering (Coulter Sub-Micron Particle Analyzer N4SD with 4 mW helium-neon laser and 90 µm detector) and ζ-potential (Coulter DELSA 440 SX), respectively.

ζ-potential values of all liposomes were measured to investigate the effect of drug loading on liposomal surface charge. Liposome dispersions were diluted with TBS pH 7.40 and ζ-potentials were measured at 25°C. As the radii of liposomes were always large compared to the Debye-Huckel parameters, the ζ-potentials were calculated directly from the Helmoholtz-Smolowkovski equation (using *Zetasizer*) [16]. Size was also calculated according to Langley [19]: the autocorrelation function of scattered light was analyzed by the cumulant method [20] to obtain mean size and the polydispersity index (P.I.).

UV-visible experiments

UV-visible spectra were recorded at 25°C with a Perkin-Elmer Lambda 25 spectrophotometer, using 10 mm cuvettes. Prior to spectral recording, liposome disruption was carried out to reduce background scattering (scaling as λ^{-4}) due to large aggregates in solution that affect intensity evaluation. To disrupt liposomes and release entrapped doxorubicin, samples underwent several cycles of freezing (-32°C).

A calibration curve was constructed by measuring the absorbance of solutions with known doxorubicin concentration at 485 nm. This wavelength was chosen to optimize detection of doxorubicin [21].

NMR spectroscopy

NMR spectra of plain and loaded functionalized liposomes were acquired at 298 K on a Bruker DRX-600 AVANCE spectrometer, equipped with an *xyz* gradient unit and operating at 600.13 MHz for ^{1}H. Two dimensional NOESY spectra (8 ppm spectral width, F2=2048, F1=512 complex points)

were acquired using mixing times of 400 ms. FIDs were processed using an exponential multiple function. Water suppression for the 2D spectra was performed using the presaturation sequence.
The data was processed with Bruker XWINNMR Software, version 2 on Silicon Graphics equipped with RISC R5000 processor, working under the IRIX 6.3 operating system.

***In vitro* binding and uptake of LTL-functionalized and non functionalized liposomes**

2×10^4 DU145 and B16-F10 cells were seeded onto cover slides in 24-well culture plates or 2×10^5 cells onto 5 cm plates (Sarstedt, Nümbrecht, Germany) and incubated under standard culture conditions in EMEM supplemented with 10% FBS. LTL-Dex-L, Dex-L, LTL-Dox-L and Dox-L (stock solution diluted 1:20) were administered to the cultured cells at 50% confluence. Untreated cells were used as control. For binding experiments, the cells were incubated with liposomes for 5, 10 and 15 min, then slides containing cells were washed in DPBS and immediately observed by laser confocal microscope. For uptake experiments, the cells were incubated with liposomes for 30 min, the medium containing liposomes was discarded and the cells were grown in fresh medium in slides or on plates for different times. Slides containing cells were then processed as previously described. Images were processed by *LSM Image* software (Zeiss, Jena, Germany). Cells cultured on plates were instead trypsinized and washed in DPBS. $1x10^5$ cells of each sample and the control were resuspended in 200 µl ice-cold DPBS and analyzed in a FACScan flow cytometer (Becton Dickinson, San Jose, CA).

Growth inhibition test

2×10^5 DU145 cells were seeded in 5 cm diameter dishes in EMEM supplemented with 10% FBS and left to grow for 24 h. The media were removed and replaced with medium containing or not containing test substances (LTL-Dox-L and Dox-L) for 30 min; the medium containing liposomes was then discarded and the cells were grown in fresh medium for different times. The growth rate was evaluated after 5, 16, 24 and 36 h of incubation. Each time the cells were removed by trypsinization, washed in DPBS and counted under an inverted optical microscope. Data was expressed as the mean of the cells counted in four different experiments ± SD. Student's t-test was used to obtain *p* values.

***In vivo* administration of LTL-Dox-L**

Experiments were performed following EEC guidelines for animal care and welfare (EEC Law No. 86/609) and guidelines of the National Ethical Committee. To assess the specificity of

functionalized liposomes for cancer tissues, C57BL mice were inoculated subcutaneously in both flanks with B16-F10 (2×10^5) melanoma cells resuspended in 100 µl sterile PBS. After 15 days, when the tumor masses were palpable, mice were treated with 200 µl LTL-Dox-L suspension containing 10 µg doxorubicin by injection into the caudal vein. Control mice were treated with PBS. After 24 hours mice were sacrificed and tumors and other tissues (heart, liver and lung) were collected and embedded in Tissue-Tek O.C.T. (Sakura, San Marcos, CA), cooled in isopentane and frozen in liquid nitrogen for histological analysis. Five-µm-thick cryostat sections from tissue samples were immediately observed by confocal laser scanning microscope.

Electron microscopy

DU145 cells were processed for ultramicroscopic analysis *in situ* by flat embedding protocol, according to Rogowski et al. [22]. 2×10^4 DU145 cells were seeded onto cover slides in 24-well culture plates and incubated under standard culture conditions in EMEM supplemented with 10% FBS, left to grow for 24 h and incubated in liposomes as previously described. The medium was then gently decanted and replaced with 3% glutaraldehyde in PBS. After 5 min, the solution was replaced with 1% glutaraldehyde in PBS, and fixation continued for 1 h at RT. After a brief rinse in buffer, cells were post-fixed with buffered 1% OsO_4 for 1 h and processed by standard dehydration and flat embedding in epoxy resin. Sections were stained with uranyl acetate and lead citrate and examined in a Philips CM200-FEG transmission electron microscope (TEM). For analysis of the liposome suspension, a small drop of sample was deposited on carbon coated grids, allowed to settle for approximately one minute, and then covered with a small drop of 2% uranyl acetate. After a few seconds the sample was viewed by electron microscope. For negative staining a drop of a water-diluted suspension of liposomes (about 0.05 mg/mL) was placed on a 200-mesh formvar copper grid, allowed to adsorb and the surplus removed with filter paper. A drop of 2% (w/v) aqueous solution of uranyl acetate was added and left in contact with the sample for 5 minutes. The surplus water was removed and the sample dried at room conditions before examining the vesicles in a Philips CM200-FEG transmission electron microscope (TEM).

RESULTS

Binding and uptake of LTL by DU145 cells

We first compared the surface localization of glycans positive to the lectin from *Lotus tetragonolobus* (LTL) to that of those recognized by the lectin from *Aleuria aurantia* (AAL) which prevalently recognizes alpha-1,6-linked fucose in N-glycans in the cell line DU145. As a more generalist lectin, we used ConA from *Canavalia ensiformis* that recognizes all N-glycan structures except those bearing alpha-1,3-linked core fucose residues. The analysis was performed by incubating non permeabilized, paraformaldehyde-fixed cells with different biotinylated lectins and then detecting the lectin-positive molecules with streptavidin bound to a fluorochrome. Analysis confirmed a distribution of the LTL-positive sites similar to that previously described in CVEC cells [14]. Bright fluorescence was restricted to a single area in small cells (Figure 1 A) or a maximum of two or three areas in larger ones, and positivity was completely abolished by 0.2 M fucose. Analysis of the AAL and ConA binding sites highlighted the specificity of the LTL-positive sites. Indeed, AAL (Figure 1 B) and ConA positivities were abundantly expressed everywhere and were detectable with a lectin concentration one tenth (2.5 μg/ml) of that used to detect LTL positivity (25 μg/ml). *Lotus tetragonolobus* lectin was then confirmed to enter the cells after binding to external fucosylated glycans and to do so by an unconventional transport mechanism, as in CVEC cells. *In vitro* incubation of the cells with LTL for different time intervals, followed by fixing and detecting LTL with streptavidin-conjugated fluorochrome, prevalently localized LTL along radial rows converging to the nuclear region within 8 hours, with partial accumulation of the lectin around the nucleus within 24 hours (Figure 1 C). The same result, though with less signal brightness, was obtained by directly localizing LTL-positive glycans with fluorescein-conjugated LTL. Positivity was completely abolished by 0.2 M fucose. Conventional uptake appearing as punctate fluorescence in the cytoplasm within 8 hours and strong accumulation in the nuclear region within 24 hours was instead observed when the cells were analyzed for AAL (Figure 1 D) and ConA (Figure 1 E) uptake. The percentage of LTL taken up by the cells was also completely different to that of ConA and AAL. Indeed, the percentage of LTL was 0.004% and that of ConA and AAL was 2%. Calculation was done by densitometry, using *Quantity one* software to analyze the reactive bands obtained in the lectin blot with lysates of cells incubated for 3 hours in the lectins. In order to investigate lectin uptake for dependence on dynamin, the cells were treated with Dynasore before and during lectin administration. This noncompetitive inhibitor of dynamin GTPase activity blocks dynamin-dependent endocytosis in cells [23]. The results proved that while AAL and ConA are taken up by an endocytotic mechanism apparently dependent on dynamin, LTL uptake is independent of this factor. An identical fluorescence pattern was observed after LTL administration in the presence (Figures 2S A) or absence of Dynasore (Figure 2S A1) and fluorescence less bright (Figure 2S B)

than that of controls (Figure 2S B1) after AAL and ConA administration. When tested on other cancer cells, such as murine melanoma cell line B16-F10, LTL confirmed its capacity to identify the presence and limited location of alpha-1,2-linked fucosylated epitopes at the surface of cells and to be taken up by an unconventional endocytotic mechanism.

Formulation and analysis of LTL functionalized liposomes

The mean diameters, polydispersity indexes and ζ-potential of the DOPC/DOPE liposomes (L) with and without lectin and FITC-dextran (Table 1) suggest that insertion of LTL and Dex into liposomes led to an increase in the mean diameter of vesicles. Liposomes did not change their surface charge as indicated by ζ-potential values when loaded.

The mean sizes and surface charges of liposomes synthesized with and without lectin and doxorubicin (Table 2 and Table 2S for extrusion with 50 and 100 nm membranes, respectively) indicated that vesicle diameter did not change significantly after addition. The low polydispersity indexes of plain and functionalized systems revealed that liposomes were not substantially altered by interaction with either protein or drug. Indeed, synthesized liposomes remained fairly monodispersed.

This clearly demonstrated that the lectin used to functionalize the liposomes did not affect their chemical structure. Plain DOPC/DOPE liposomes had a small positive ζ-potential, though the net polar head charge of zwitterionic phospholipids is zero. Indeed, liposomes made by other chemicals behave as slightly negative aggregates in the presence of an external electric field [24]. This may be due to preferential absorption of OH^- ions from the water environment or to outward exposure of phosphate groups. On addition of doxorubicin, the surface charge of LTL-L did not change substantially.

UV-visible analysis was carried out after the encapsulation step to determine the amount of Dox in the liposomes and the initial and loaded concentrations of doxorubicin (Tables 2 and Table 2S). The doxorubicin was correctly inserted in the synthesized liposomes. The entrapment efficiency of liposomes was calculated by the following equation: $EE\ (\%) = (C/T) \times 100$, where T is total amount of drug and C is the amount of encapsulated drug in the liposome formulation. Encapsulation efficiency tended to increase in the presence of LTL, which did not change chemical-physical properties, such as fluidity of the phospholipid bilayer, and the encapsulated drug leaked out of the liposome. Membrane fluidity was a major factor affecting encapsulation efficiency of the drug [25]. Unsaturated phospholipids increased membrane fluidity, which is expected to facilitate drug leakage [26].

Table 3 shows the diameter and polydispersity index of empty and functionalized liposomes with and without doxorubicin in relation to storage time (0, 1 and 3 months). Pure liposome diameters

were slightly larger than 100 nm, which did not change in relation to storage time. For all other formulations, liposome size and polydispersity did not show any essential variations due to chemical and physical degradation processes. These findings confirm the stability of the liposomal formulation; in particular, insertion of Dox in pure and functionalized liposomes did not modify their stability properties.

The NMR spectrum of the pure liposomes (Figure 3S A) showed proton signals of phospholipid polar heads at 3.3 ppm, as well as those of alkyl chains at 1.4 and 0.9 ppm, whereas the Dox-loaded-functionalized liposome spectra showed the same, but broader, signals. Peak assignment for DOPC/DOPE liposomes has already been reported [27]. Proton signals of most aggregated systems broadened beyond detection due to longer diffusion times and because the molecular order in the bilayer prevented complete averaging out of dipolar interactions. The observed broadening was therefore associated with interactions with lectin and doxorubicin. Since it was not possible to detect preferential broadening of the polar heads or the alkyl chain signals, this effect was attributed to growth of the overall aggregates. The inclusion of lectin in a liposome formulation is a fundamental step for improving doxorubicin loading and transport. The NMR spectrum of lectin-functionalized liposomes showed that the protein does not substantially modify liposome structure.

To evaluate the interaction processes in liposome systems, we recorded the ^{1}H spectrum of doxorubicin in D_2O (range 0-4.5 ppm) (Figure 3S C). Proton signal assignment, based on COSY, TOCSY and NOESY spectra, was in line with literature data [28] (spectra not shown). The signals at 7.70, 7.57 and 7.42 ppm were assigned to aromatic protons (H2, H1 and H3). The signals at 4.19, 3.60 and 1.24 ppm were due to protons H5', H2' and H6' (methyl group), respectively. In Figure 3S B the presence of the signals H5' and H6' of doxorubicin in the LTL-Dox-L spectrum suggests correct inclusion of the drug in the liposome structure.

The NMR resonances of doxorubicin in the presence of DOPC/DOPE liposomes were attributed to doxorubicin exchange between a free state in solution and a membrane-bound state, which caused line broadening of the spectrum without significantly changing the chemical shifts. The supposed interaction between doxorubicin and liposomes was investigated by NOESY spectra, with the aim of emphasizing differences in the dipolar interactions occurring in aqueous solution or in the presence of liposomes.

The two dimensional NOESY experiment to reveal spatial relationships between proximal protons was applied to liposome systems to study structural details of proton-proton interaction. NOESY cross-peaks indicated proximity (<4.5 Å) of the lipid protons and the protons of doxorubicin, and the size of NOE was inversely dependent on the distance between interacting spins.

The first evaluation of the NOESY spectrum of LTL-Dox-L (Figure 2) indicated that cross-peaks with the same sign showed as diagonal peaks. This depends on the rotational correlation time of the

molecule embedded in the aggregates [29]. In particular, if the rotational correlation time of the molecules is long (i.e. τ_c 3×10^{-10}s), diagonal and cross-peaks have same sign. This meant that doxorubicin molecules were in slow motion conditions with the liposomes.

Dipolar couplings were evident between H5' (4.18 ppm) and H2' (3.45 ppm) of doxorubicin and the protons H6 of the DOPC polar head (3.12 ppm), indicating that drug was intercalated in the liposome bilayer. The doxorubicin aromatic part was directly involved in this process, possibly in close contact with the lipid chain. The polar head groups of lipids (H6) behaved as a tethering point for the doxorubicin pyranosyl group.

Intracellular uptake of LTL-Dex-L and Dex-L in the cancer cell line DU145

We first analyzed the efficiency of liposomes in targeting DU145 cells by fluorescently labeling them with the water-soluble Dex, a very hydrophilic marker that is practically unable to penetrate cells except by liposome endocytosis. Confocal microscopy of cells incubated in 100 nm and 50 nm membrane-extruded LTL-Dex-L and Dex-L for different time intervals revealed that 100 and 50 nm targeted liposomes were internalized more efficiently than non targeted ones of similar diameter. As variability in the uptake of the 50 nm targeted liposomes was consistently lower than that of 100 nm ones, the remaining analyses used 50 nm liposomes. Cells incubated with these liposomes for different time intervals showed that the latter were internalized by a very unconventional mechanism. As shown in Figure 3, the fluorescence due to Dex appeared as extremely bright spots distributed along evident tubule structures converging to the nuclear region (Figure 3 A). Very faint fluorescence was detectable on cells incubated with non functionalized liposomes (Figure 3 B).

Binding and intracellular uptake of LTL-Dox-L and Dox-L in DU145 cells

We then encapsulated doxorubicin in liposomes and analyzed binding of LTL-Dox-L and Dox-L by confocal microscopy. The analysis was first performed by incubating non permeabilized, paraformaldehyde-fixed cells with liposomes for 5, 15 and 30 min. At all time intervals and with both types of liposomes, fluorescence due to doxorubicin was only found in the nucleus. We then incubated the cells in the liposomes for 5 min, washed them and immediately observed them under the microscope without any other treatment. In this case we observed a fluorescence pattern due to doxorubicin restricted to small areas on the cell surface (Figure 4 A); the pattern was similar to that observed after *Lotus* lectin administration. When Dox-L was used, we found faint fluorescence in the nucleus instead. These results suggested that paraformaldehyde treatment of the cells somehow influences LTL-functionalized liposome stability. We therefore decided to conduct all other experiments using living cells.

To analyze liposome internalization we observed the cells 6, 16, 24 and 36 hours after liposome

administration and by FACS 16 and 24 hours after vesicle administration to the cells. Six hours with targeted liposomes gave rise to faint spotted red fluorescence due to doxorubicin at the cell periphery. After 16 hours of incubation, very bright spots distributed like those for LTL-Dex-L were observed. Red fluorescence was prevalently disposed in regular rows, sometimes resembling tubules converging on the nucleus (Figure 4 B). No fluorescence was associated with the cytoplasm of cells incubated for the same time in Dox-L (Figure 4 C). In this case, faint fluorescence was only observed in the nuclei. After 24 hours of incubation, differential localization of doxorubicin encapsulated in LTL-Dox-L and Dox-L was confirmed. All red fluorescence appeared concentrated around the nuclear region in cells incubated in targeted liposomes (Figure 4S), whereas when Dox-L was used, fluorescence remained completely restricted to the nucleus. FACS analysis of the same cells incubated in LTL-Dox-L and Dox-L for 16 and 24 hours confirmed greater fluorescence associated with cells incubated in functionalized liposomes than with cells incubated in non functionalized liposomes at both times (16 h Figure 4 D; 24 h Figure 4S).

After 36 hours of incubation, there were fewer adherent cells than after 24 hours, and they showed greater signs of damage, such as evident vacuoles. The red fluorescence of doxorubicin concentrated in large bodies close to the nucleus of cells incubated in functionalized liposomes (Figure 5 A). Fluorescence persisted in the nucleus of cells incubated in non functionalized liposomes (Figure 5 B). Dependence of LTL-Dox-L uptake on the LTL insertion was tested by incubating cells in the lectin before and during incubation of the cells with liposomes, then washing the cells, allowing them to grow for three hours in the medium and then measuring their fluorescence with a spectrofluorimeter. The results confirmed the importance of the lectin in targeting liposomes to cells, since 60% lowering of red fluorescence with respect to control was obtained with a lectin concentration of 100 μg/ml.

To further investigate the endocytotic mechanism by which LTL-Dox-L was taken up by DU145, cells incubated in LTL-Dox-L or Dox-L for 16 hours were fixed, flat embedded and analyzed by electron microscope. As reported in Figure 6 A and B round structures of about 40-50 nm resembling liposomes were always observed intact and lined up one by one inside tiny tubular membranous structures. Many coated vesicles were observed at the cell surface but liposomes were never found inside them (Figure 5S). Large vesicles with many liposomes still intact or partially fused were observed in a few sections close to the nucleus (Figure 6 B and insert). No structures resembling liposomes were observed inside the cells when Dox-L was used. Confirmation that the structures identified in the LTL-Dox-L incubated cells were liposomes was acquired by negative staining of a liposome suspension. As observed in the insert of Figure 6 A, isolated liposomes appear as spherical structures with a diameter of about 30-40 nm, like those observed in the cell tubules. The electron and confocal microscope findings indicate that LTL-targeted liposomes

entered the cells and traveled inside them via a system of fine tubules that conveyed them to large vesicles in the nuclear region, where they could fuse without releasing the encapsulated doxorubicin.

Growth rate inhibition of LTL-Dox-L and Dox-L in DU145 cells

Finally we investigated whether incubation of cells in LTL-Dox-L and Dox-L influenced cell proliferation. The growth rate of DU145 measured while incubating the cells in liposomes was compared with that of cells incubated without liposomes. Growth rate was evaluated by counting cells at different time intervals of liposome incubation (Figure 7). After 5 hours of incubation, liposome-treated cells were not found to differ in number from control cells ($p>0.05$). After 16, 24 and 36 hours of incubation, the number of treated cells with functionalized and non functionalized liposomes decreased progressively and significantly ($p<0.05$), while that of control cells progressively increased.

Intracellular uptake of LTL-Dox-L and Dox-L by murine cancer cell line B16-F10

In order to determine whether functionalized liposomes were also internalized by cancer cell lines other than DU145, they were administered to cells of the murine melanoma cell line B16-F10. In this case the liposomes were administered for 6, 16 and 24 hours. Confocal microscopy confirmed that 16-hour incubation resulted in strong red fluorescence close to the nucleus when functionalized liposomes were administered (Figure 8 A) and very faint dispersed red fluorescence when non functionalized liposomes were used (Figure 8 B). In cells with targeted liposomes, red fluorescence due to doxorubicin persisted in the liposomes and concentrated in a sharp triangular region protruding towards the nucleus.

LTL-Dox-L localization in tumors

The efficacy of LTL-Dox-L in targeting tumors was determined by injecting B16-F10 cells subcutaneously into mice, and then treating them with liposomes containing 20 μg Dox equivalent per tumor. The mice were sacrificed 24 hours later. Tumor and other tissue sections were analyzed by confocal fluorescence microscopy. Bright red fluorescence was observed inside the tumor cells (Figure 9 A and B), whereas no fluorescence was found in other tissue sections (Figure 9 C), suggesting that liposome functionalization also allows cell internalization *in vivo*. This result was in line with internalization by B16-F10 cells observed *in vitro.*

DISCUSSION

Active targeting by conjugation of ligands with the surface of liposomes has been explored to enhance the specificity and efficacy of drug delivery to diseased tissues and cells, as well as drug retention without deposition in non target-sites. Many different classes of ligands have been used for this purpose. Since the discovery that folate [30] and transferrin [31] receptors are overexpressed at the surface of many cancer cells, these moieties became the first target molecules and are still widely studied. Immunoliposomes coupled with monoclonal antibodies against cancer-specific surface proteins are also versatile, widely used ligands. However, despite many positive results, clinical translation of known targeted liposomes has not progressed in a corresponding manner [32]. The search for new more efficient drug delivery systems therefore continues.

In this study we constructed liposomes functionalized with the lectin derived from *Lotus tetragonolobus.* Compared to non targeted liposomes, these highly stable liposomes specifically bind and efficiently enter target cells *in vitro* and *in vivo* and target a surface glycoepitope only expressed in cells with aberrant cell growth, a hallmark of cancer [14].

Lotus tetragonolobus lectin was found to efficiently direct liposomes into cells by a pathway identical to that of the lectin but different to that of other lectins. Although unlike dextran, doxorubicin can cross the membranes, it is interesting that neither encapsulated molecule was ever delivered by LTL-Dox-L, nor did doxorubicin accumulate in the nucleus or in other organelles in the 36 hours after incubation with targeted liposomes. Electron and confocal microscopy indicated that although the liposomes fused in the final vesicles that hosted them in the nuclear region, doxorubicin remained bound to them. The drug delivery mechanism of the same liposomes without the lectin was completely different. We postulate that they fuse with the plasma membrane, immediately releasing the encapsulated drug, since they were never detected in the cytoplasm by electron microscopy or confocal microscopy, whereas doxorubicin appeared in the nucleus 5 minutes after incubation of cells with Dox-L.

Targeted Dox-loaded liposomes are reported to enter cells predominantly by a receptor-ligand mediated interaction that includes: clathrin-mediated vesicle formation [33], passage into acidic endosomal compartments that degrades the nanocarriers, and drug delivery to the nucleus [34]. Vesicle-mediated endocytosis [35] and lysosomal passage [36] have also been reported for lectin-functionalized liposomes. The independence of LTL uptake from dynamin, along with the incapacity of doxorubicin encapsulated in LTL-targeted liposomes to be released and to reach the nucleus, as well as the shape of the structures in which the liposomes travel, exclude the possibility that LTL-Dox-L uses a clathrin-dependent route or other systems that include lysosomal passage as endocytic mechanism. Electron microscopy confirmed clathrin-independence of LTL-liposome

uptake, since LTL-liposomes were never found in coated vesicles or in lysosomal organelles. Further work is necessary to understand the parameters of this new uptake mechanism, although recently reported clathrin- and caveolin-independent endocytic pathways involving formation of tubules instead of vesicles are suggested to be a primordial endocytic system [37]. Unfortunately characterization of this mechanism is still in its infancy.

Although not delivered to the nucleus, doxorubicin encapsulated in LTL-Dox-L was found to exert cytotoxic activity similar to that of the drug that reaches the nucleus from Dox-L. It can therefore be deduced that the antiproliferative action of Dox in LTL-Dox-L cannot include the mechanisms proposed for this drug at nuclear level, such as topoisomerase II inhibition, DNA intercalation [38] and free radical generation, but instead may act according to the mechanism proposed by Denard, Lee and Ye [39], known as *regulated intramembrane proteolysis*. In this process, a membrane-bound protein is cleaved, releasing a soluble messaging molecule that can play a role in a variety of cell processes, including apoptosis. The stability, targeting efficiency, targeting specificity and peculiar internalization pathway of LTL-targeted liposomes were also demonstrated *in vivo*, since liposomes injected into mice with induced melanomas reached their target without being internalized by cells of other tissues.

CONCLUSIONS

We designed doxorubicin-loaded DOPC/DOPE liposomes functionalized with a glycoprotein (lectin from *Lotus tetragonolobus*) that efficiently delivers the drug to cancer cells with specific characteristics by a specifically delineated intracellular trafficking mechanism. Doxorubicin-LTL functionalized liposomes promise to be useful in the development of new cancer chemotherapy protocols.

Acknowledgements

The authors thank the University of Siena.

Declarations of interest

The authors report no declarations of interest.

Conflict of interest

The authors declare that they have no conflicts of interest.

BIBLIOGRAPHY

[1] V.P. Torchilin, Recent advances with liposomes as pharmaceutical carriers, Nat. Rev. Drug Discov. 4 (2005) 145-160.

[2] S. Rivankar, An overview of Doxorubicin formulation in cancer therapy, J. Cancer Res. Ther. 10 (2014) 853-858.

[3] L. Rajendran, H.J. Knolker, K. Simons, Subcellular targeting strategies for drug design and delivery, Nat. Rev. Drug Discov. 9 (2010) 29-42.

[4] G. Batist, G. Ramakrishnan, C.S. Rao, A. Chandrasekharan, J. Gutheil, T. Guthrie, P. Shah, A. Khojasteh, M.K. Nair, K. Hoelzer, K. Tkaczuk, Y.C. Park, L.W. Lee, Reduced cardiotoxicity and preserved antitumor efficacy of liposome-encapsulated Doxorubicin and cyclo phosphamide compared with conventional Doxorubicin and cyclo phosphamide in a randomized multicenter trial of metastatic breast cancer, J. Clin. Oncol. 19 (2001) 1444-1454.

[5] E. Tahover, Y.P. Patil, A.A. Gabizon, Emerging delivery systems to reduce Doxorubicin cardiotoxicity and improve therapeutic index: focus on liposomes, Anticancer Drugs 26 (2015) 241-258.

[6] J. Conniot, J.M. Silva, J.G. Fernandez, L.C. Silva, R. Gaspar, F. Brocchini, H.F. Florindo, T.S. Barata, Cancer immunotherapy: nanodelivery approaches for immune cell targeting and tracking, Front. Chem. 2 (2014) 105-132.

[7] H. Ghazarian, B. Idoni, S.B, Oppenheimer, A glycobiology review: carbohydrates, lectins, and implications in cancer therapeutics, Acta Histochem. 113 (2011) 236-247.

[8] M.N. Christiansen, J. Chik, L. Ling, M. Anugrahm, J.L. Abrahams, N. Packer, Cell surface protein glycosylation in cancer, Proteomics 14 (2014) 525-546.

[9] A.S. Powlesland, P.G. Hitchen, S. Parry, S.A. Graham, M.M. Barrio, M.T. Elola, J. Mordoh, A. Dell, K. Drickamer, M.E. Taylor, Targeted glycoproteomic identification of cancer cell glycosylation, Glycobiology 19 (2009) 899-909.

[10] S.R. Stowell, T. Ju, R.D. Cummings, Protein glycosylation in cancer, Ann. Rev. Pathol. 10 (2011) 473-510.

[11] C.A. Roney, B. Xu, J. Xie, S. Yuan, J. Wierwille, C.W. Chen, G.L. Griffiths, R.M. Summers, Rh-I-UEA-1 polymerized liposomes target and image adenomatous polyps in the APC(Min/+) mouse using optical colonography, Mol. Imaging 10 (2011) 305-316.

[12] F. Gabor, E. Bogner, A. Weissenboech, M. Virth, The lectin-cell interaction and its implications to intestinal lectin-mediated drug delivery, Adv. Drug Deliv. Rev. 56 (2004) 459-480.

[13] V. Gajbhiye, S. Gong, Lectin functionalized nanocarriers for gene delivery, Biotechnol. Adv. 31 (2013) 552-562.

[14] S. Aldi, A. Capone, C. Della Giovampaola, L. Ermini, E. Pianigiani, G. Mariotti, F. Rosati, Identification of a novel, alpha2-fucosylation-dependent uptake system in highly proliferative cells, Tissue Cell 47 (2015) 33-38.

[15] C. Bonechi, S. Martini, L. Ciani, S. Lamponi, C. Setzer, H. Rebmann, C. Rossi, S. Ristori, Using liposomes as carriers for polyphenolic compounds: the case of trans-resveratrol, PloS One 7 (2012) e41438. doi: 10.1371.

[16] R. J. Hunter, Zeta Potential in Colloid Science: Principles And Application, (Academic Press, UK) (1988).

[17] U.K. Laemmli, Cleavage of structural proteins during the assembly of the head of the bacteriophage T4, Nature 27 (1970) 680-685.

[18] G. Leone, M. Consumi, S. Lamponi, A. Magnani, New hyaluroran derivative with prolonged half-life for ophthalmogical formulation, Carbohydrate Polymers 88 (2012) 799-808.

[19] K.H. Langley, Developments in electrophoretic laser light scattering and some of biochemical applications, in: S.E. Harding, D.B. Sattelle, V.A. Bloomfield (Eds.), Laser Light Scattering in Biochemistry, The Royal Society of Chemistry (1992) pp. 151-160.

[20] D.E. Koppel, Analysis of Macromolecular Polydispersity in Intensity Correlation Spectroscopy: The Method of Cumulants, Journal of Chemical Physics 57 (1972) 4814-4820.

[21] C.S.P. Sastry, J.S.V.M. Lingeswara Rao, Determination of Doxorubicin hydrochloride by visible spectrophotometry, Talanta 43 (1996) 1827-1835.

[22] M. Rogowski, D. Scholz, S. Geimer, Electron Microscopy of Flagella, Primary Cilia, and Intraflagellar Transport in Flat-Embedded Cells, Methods Enzymol. 524 (2013) 243-263.

[23] T. Kirchhausen, E. Macia, H.E. Pelish, Use of dynasore, the small molecule inhibitor of dynamin, in the regulation of endocytosis, Methods Enzymol. 438 (2008) 77-93.

[24] G. Cevc, Electrostatic characterization of liposomes, Chemistry and Physics of Lipids, 64 (1993) 163-186.

[25] S.B. Kulkarni, G.V. Betageri, M. Singh, Factors affecting microencapsulation of drugs in liposomes, J. Microencapsul. 12 (1995) 229-246.

[26] N. Tomoko, I. Fumiyoshi, Encapsulation efficiency of water-soluble and insoluble drugs in liposomes prepared by the microencapsulation vesicle method, Int. J. Pharm. 298 (2005) 198-205.

[27] C. Bonechi, S. Ristori, G. Martini, S. Martini, C. Rossi, Study of bradykinin conformation in the presence of model membrane by Nuclear Magnetic Resonance and molecular modeling, Biochim. Biophys. Acta. 1788 (2009) 708-716.

[28] C. Chun, S.M. Lee, C.W. Kim, K.Y. Hong, S.Y. Kim, H.K. Yang, S.C. Song, Doxorubicin-polyphosphazene conjugate hydrogels for locally controlled delivery of cancer therapeutics, Biomaterials 30 (2009) 4752-4762.

[29] M.H. Levitt, Basic of nuclear magnetic resonance, John Wiley and Sons, New York, 2001.

[30] Y. Lu , P.S.Low, Folate-mediated delivery of macromolecular anticancer therapeutic agents, Adv Drug Deliv Rev 54 (2002) 675–693.

[31] R. Sutherland , D. Delia, C. Schneider, R. Newman, J. Kemshead, M. Greaves, Ubiquitous cell-surface glycoprotein on tumor cells is proliferation-associated receptor for transferring, Proc. Natl. Acad. Sci. U S A. 78 (1981) 4515–4519.

[32] L. Sercombe, T. Veerati, F. Moheimani, S.Y. Wu, A.K. Sood, S. Hua, Advances and challenges of liposome assisted drug delivery, Front. Pharmacol. 6 (2015) 286-289.

[33] F. Gabor, E. Bogner, A. Weissenboeck, M. Wirth, The lectin-cell interaction and its implications to intestinal lectin-mediated drug delivery, Adv. Drug Deliv. Rev. 56 (2004) 459-480.

[34] G. Sahay, D.Y. Alakhova, A.V. Kabanov, Endocytosis of nanomedicines, J. Control. Release. 145 (2010) 182-195.

[35] A. Brück, R. Abu-Dahab, G. Borchard, U.F. Schäfer, C.M. Lehr, Lectin-functionalized liposomes for pulmonary drug delivery: interaction with human alveolar epithelial cells, J. Drug Target 9 (2001) 241-251.

[36] L. Neutsch, V. E. Plattner, S. Polster-Wildhofen, A. Zidar, A. Chott, G. Borchard, O. Zechner, F. Gabor, M. Wirth, Lectin mediated biorecognition as a novel strategy for targeted delivery to bladder cancer, J. Urol. 186 (2011) 1481-1488.

[37] M. Satyajit, R.E. Pagano, Pathways of clathrin-independent endocytosis, Nat. Rev. Mol. Cell. Biol. 8 (2007) 603-612.

[38] C.F. Thorn, C. Oshiro, S. Marsh, T. Hernandez-Boussard, H. McLeod, T. E. Klein, R. B. Altman, Doxorubicin pathways: pharmacodynamics and adverse effects, Pharmacogenet. Genomics 21 (2011) 440-446.

[39] B. Denard, C. Lee, J. Ye, Doxorubicin blocks proliferation of cancer cells through proteolytic activation of CREB3L1, eLife Sciences 1 (2012) e00090 doi: 10.7554/eLife.00090.

LEGEND OF FIGURES

Figure 1. Representative confocal images of LTL (A) and AAL (B) binding and 12-hour uptake of LTL (C), AAL (D) and ConA (E) by DU145 cells. Non permeabilized, paraformaldehyde-fixed cells were tested with 25 μg/ml LTL and 2.5 μg/ml AAL. Positive molecules were detected with streptavidin bound to Alexa Fluor 488. Fluorescence (A and B), light (A1 and B1) and merged (A2 and B2) images. For uptake, cells were incubated with 25 μg/ml LTL (A) and 2.5 μg/ml AAL (B) and ConA (C) for 1 hour then the lectins were removed and the cells left in culture for 11 hours. Cells were then fixed and positive molecules detected with streptavidin bound to Alexa Fluor 488.

Figure 2. 2D NOESY spectrum of DOPC/DOPE incorporated with LTL and Dox at 298 K in D_2O. The major cross-peaks are: a) 4.18-3.45 ppm (H5' Dox-H2' Dox); b) 4.18-3.12 ppm (H5' Dox-H6 DOPC); c) 3.45-3.12 ppm (H2' Dox-H6 DOPC).

Figure 3. Representative confocal images of DU145 cells treated for 16 hours with LTL-Dex-L (A) and Dex-L (B). Cells were incubated with the liposomal suspension for 30 minutes, then the liposomes were removed and the cells left in culture for 16 hours.

Figure 4. Representative confocal image of LTL-Dox-L binding to DU145 cancer cells (A) and 16-hour uptake of LTL-Dox-L (B) and Dox-L (C) in cancer cells of the DU145 line, detected by confocal microscope and flow cytometry (D). For binding, cells were incubated for 5 minutes in the liposomal suspension and immediately observed. For uptake, cells were incubated with the liposomal suspension for 30 minutes, then the liposomes were removed and the cells left in culture for 16 hours. The flow cytometry histograms were obtained from a single experiment representative of three similar experiments.

Figure 5. Thirty-six-hour uptake of LTL-Dox-L (A) and Dox-L (B) in cancer cells of the DU145 line detected by confocal microscope. Cells were incubated with the liposomal suspension for 30 minutes, then the liposomes were removed and the cells left in culture for 36 hours.

Figure 6. Uptake of LTL-Dox-L by DU145 cells for 16 hours detected by electron microscope. Cells incubated in LTL-Dox-L for 30 minutes and left in culture for 16 hours were flat embedded, sectioned, stained and examined by electron microscope. Liposomes lined up one by one in tiny tubules (arrows) (A and B) and once close to the nuclear region were observed in large vesicles (B) where some also fused (B, Insert). Negative staining of a LTL-Dox-L suspension (A, Insert).

Figure 7. Growth curve of DU145 cells incubated in LTL-Dox-L and Dox-L. Cells were incubated with or without liposomes and counted at the time intervals indicated. The graph shows the average of four independent experiments. Mean data from four independent experiments ± SD. Error bars are shown for each group; $p>0.05$ at 5 h; $p<0.05$ at 16, 24 and 36 h.

Figure 8. Sixteen-hour uptake of LTL-Dox-L (A) and Dox-L (B) in cancer cells of the B16-F10 melanoma cancer line detected by confocal microscope. Cells were incubated with the liposomal suspension for 30 minutes, then the liposomes were removed and the cells left in culture for 16 hours.

Figure 9. Twenty-four-hour cell uptake of LTL-Dox-L *in vivo.* Fluorescence microscopy images of two sections of melanoma (A and B) and one section of heart (C), showing localization of Dox after intravenous administration of 100 µl of liposomes containing 10 µl Dox.

Table 1. Characteristics of DOPC/DOPE liposomes (L) (100 nm polycarbonate membranes) with FITC-Dextran (Dex) and lectin (LTL) without doxorubicin.

Table 2. Characteristics of DOPC/DOPE liposomes (L) (50 nm polycarbonate membranes) with and without doxorubicin (Dox) and lectin (LTL).

Table 3. Diameter and polydispersity index of the investigated liposomes *vs* storage time.

SUPPLEMENTARY MATERIAL

Figure 1S. ATR-FTIR spectra of lectin-oleic acid conjugate after purification (A) and lectin-oleic acid conjugate in water and after subtraction (B).

Figure 2S. Effect of Dynasore on LTL (A) and AAL (B) uptake. Cells were incubated with 80 µM Dynasore for 30 min, then with 25 µg/ml LTL (A) and 2.5 µg/ml AAL (B) in the presence of 80 µM Dynasore for 30 min. Lectins and Dynasore were then removed and the cells left in culture for 11 hours. Cells were then fixed and positive molecules detected with streptavidin bound to Alexa Fluor 488.

Figure 3S. NMR proton spectrum in D_2O (range 0-4.5 ppm) for DOPC/DOPE liposome, L (A),

LTL-Dox-L liposome (B) and doxorubicin (Dox) $1.5x10^{-3}$ M (C).

Figure 4S. Twenty-four-hour uptake of LTL-Dox-L (A) and Dox-L (B) in cancer cells of the DU145 line detected by confocal microscope and flow cytometry (C). Cells were incubated with the liposomal suspension for 30 minutes, then the liposomes were removed and the cells left in culture for 24 hours. The flow cytometry histograms were obtained from a single experiment representative of three similar experiments.

Figure 5S. Sixteen-hour uptake of LTL-Dox-L by DU145 cells detected by electron microscope. Cells incubated in LTL-Dox-L for 30 minutes and left in culture for 16 hours were flat embedded, sectioned, stained and examined by electron microscope. A liposome in a tubule (arrow) and a coated vesicle without liposomes (arrow head).

Table 1S. Overview of lectin-oleic acid conjugate infrared bands.

Table 2S. Characteristics of DOPC/DOPE liposomes (100 nm polycarbonate membranes) with and without doxorubicin (Dox) and lectin (LTL).

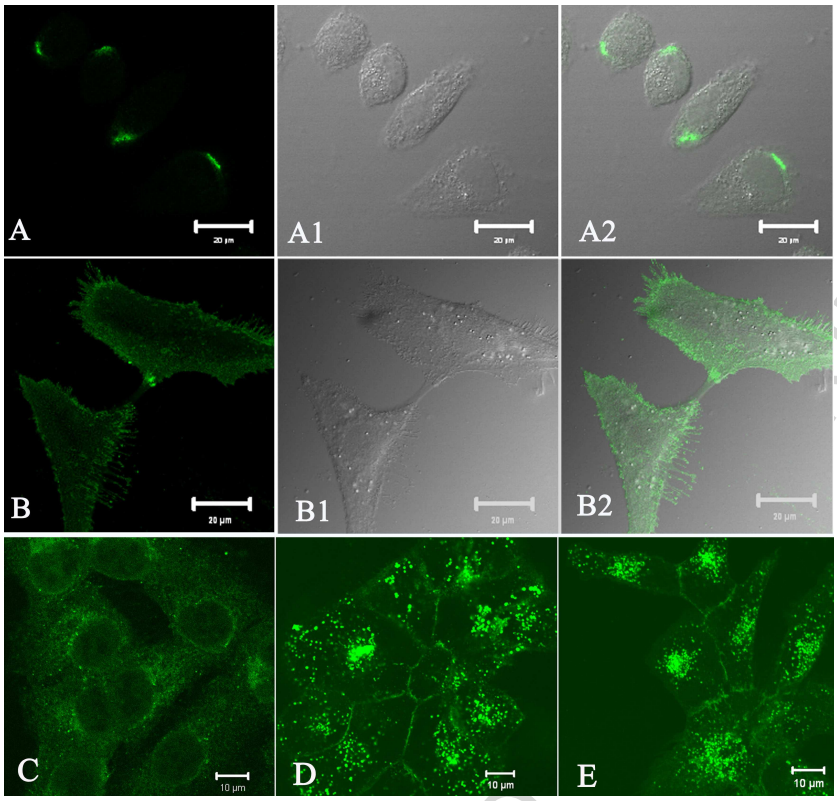

Fig. 1

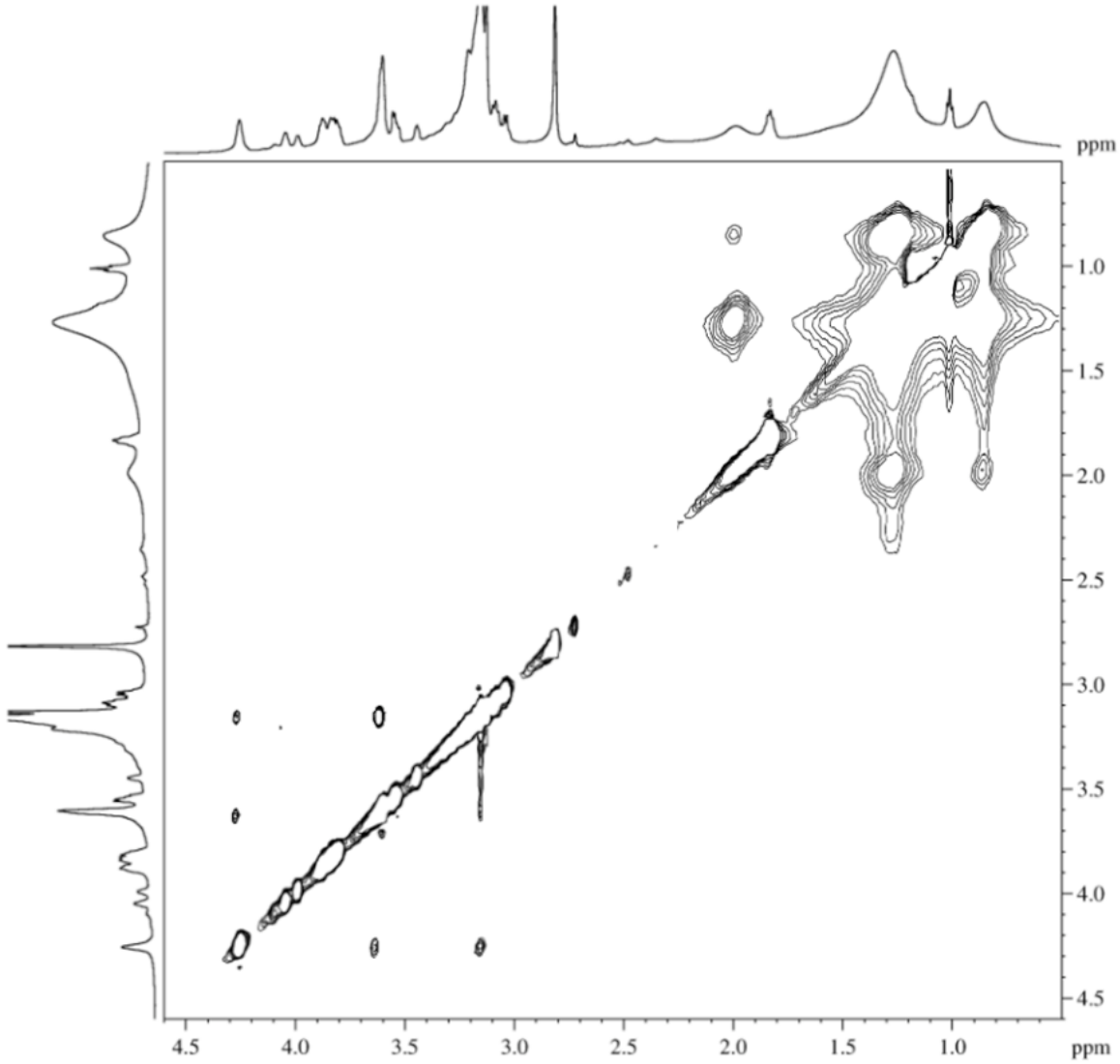

Fig. 2

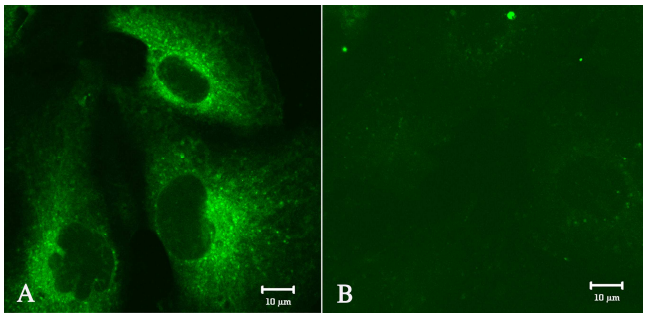

Fig. 3

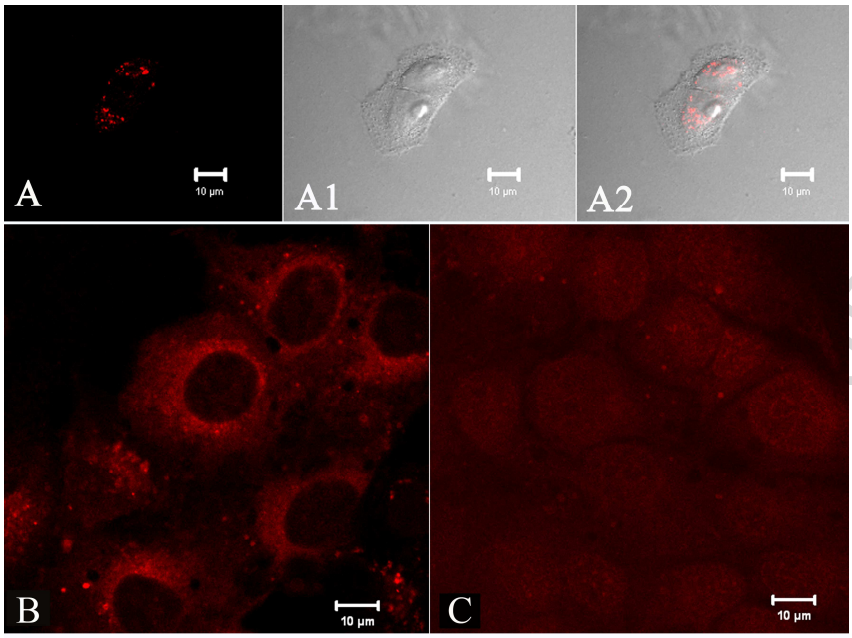

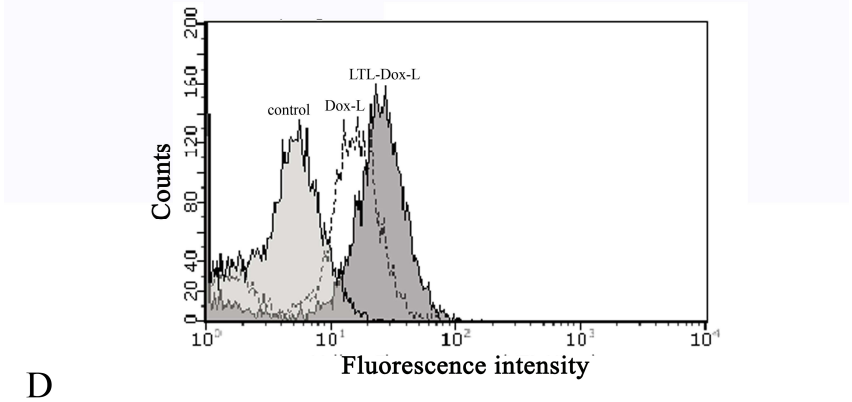

D

Fig. 4

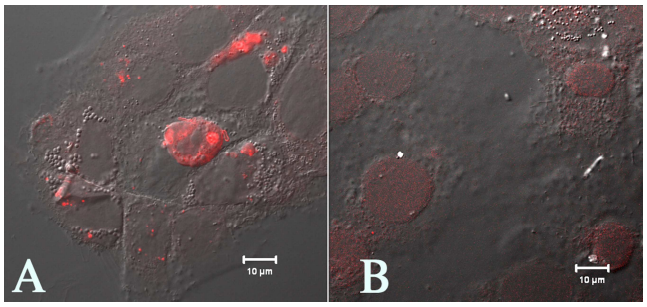

Fig. 5

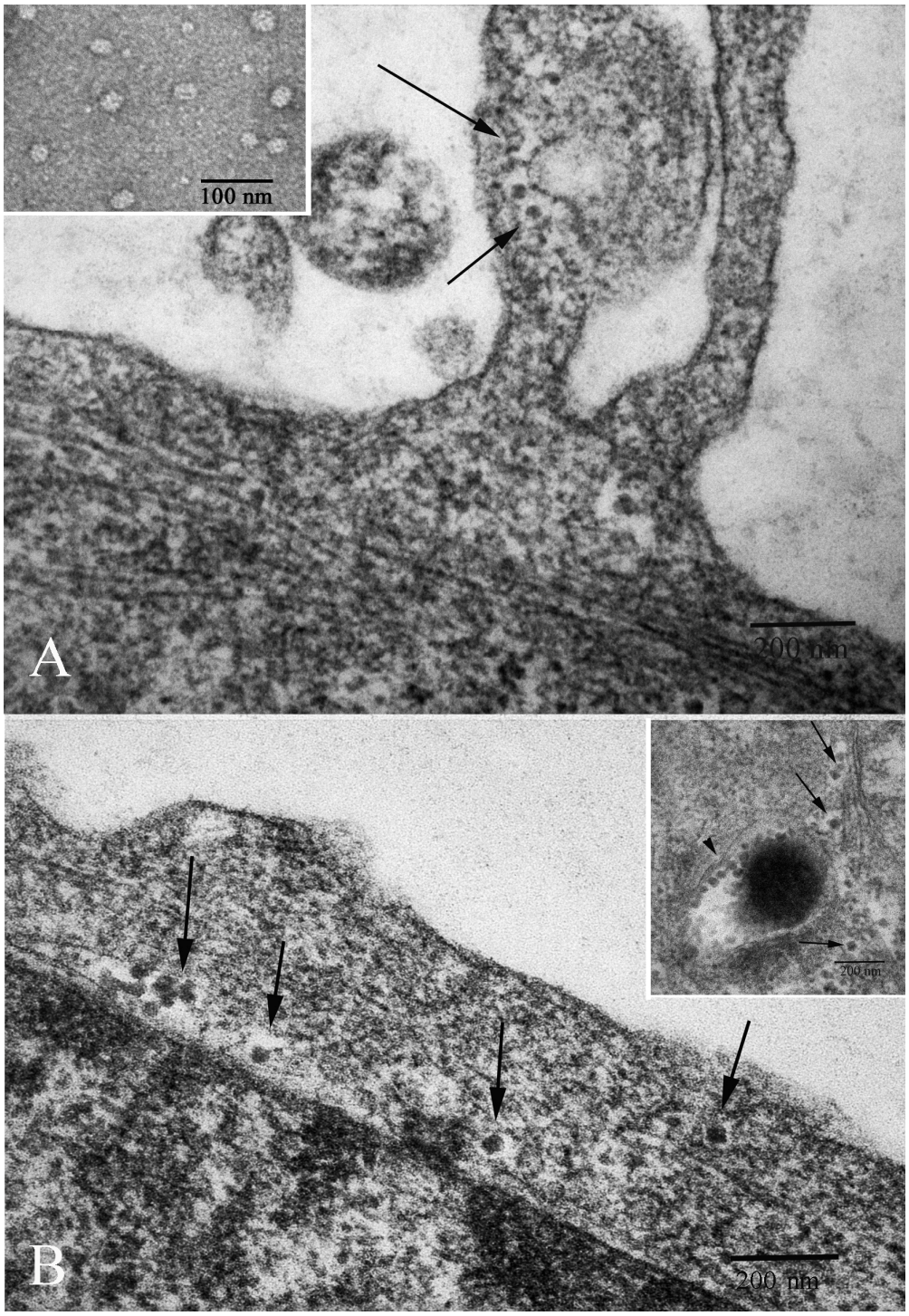

Fig. 6

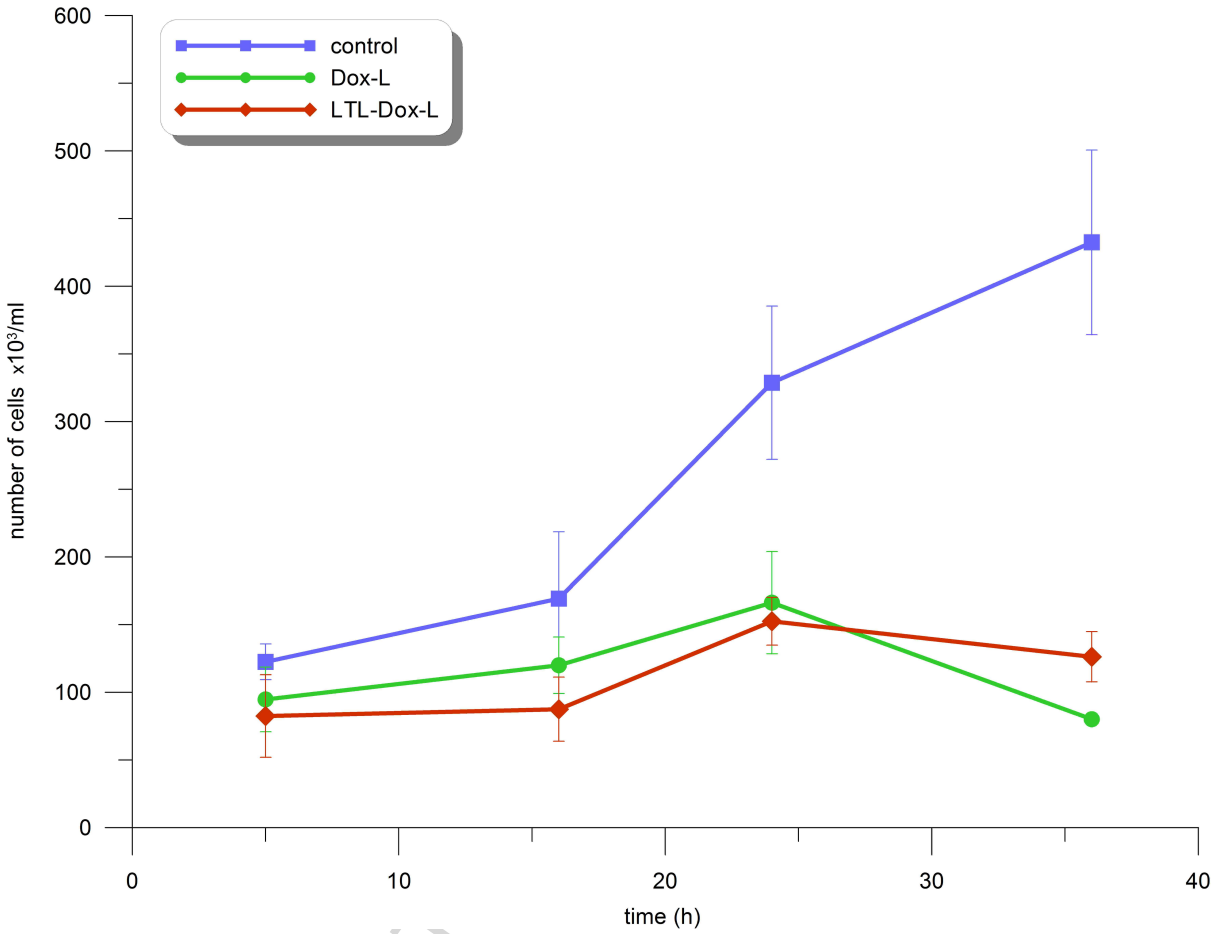

Fig. 7

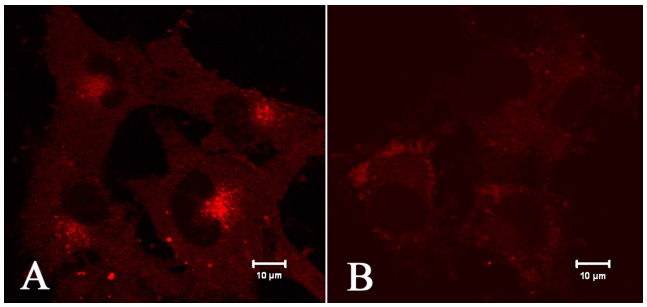

Fig. 8

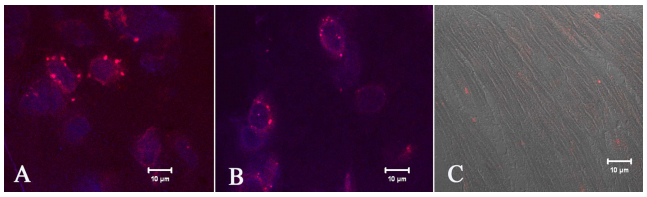

Fig. 9

Table 1. Characteristics of DOPC/DOPE liposomes (L) (100 nm polycarbonate membranes) with FITC-Dextran (Dex) and lectin (LTL) without doxorubicin.

Composition	**Mean diameter (nm)**	**P.I.**	**Zeta potential (mV)**
L (1:1)	105±13	0.05	7±3
LTL-L	127±11	0.05	-9±3
Dex-L	140±9	0.05	-3±3
LTL-Dex-L	149±7	0.04	-4±3

Table 2. Characteristics of DOPC/DOPE liposomes (L) (50 nm polycarbonate membranes) with and without doxorubicin (Dox) and lectin (LTL).

Composition	**Initial Dox concentration (M)**	**Loaded Dox concentration (M)**	**Encapsulation Efficiency EE%**	**Mean diameter (nm)**	**P.I.**	**Zeta potential (mV)**
L (1:1)	-	-		72±15	0.13	8±2
LTL-L	-	-		90±10	0.11	-11±2
LTL-Dox-L	$1.5x10^{-4}$	$8.1x10^{-5}$	54.0±6	86±15	0.12	-8±2
Dox-L	$1.5x10^{-4}$	$7.0x10^{-5}$	46.7±5	75±15	0.11	-7±3

Table 3. Diameter and polydispersity index of the investigated liposomes *vs* storage time

	0 month		1 month		3 months	
	Mean diameter (nm)	**P.I.**	**Mean diameter (nm)**	**P.I.**	**Mean diameter (nm)**	**P.I.**
L (1:1)	100±15	0.10	105±11	0.10	107±10	0.11
LTL-L	125±15	0.11	130±9	0.13	135±9	0.15
LTL-Dox-L	130±15	0.10	130±11	0.10	136±10	0.13
Dox-L	110±10	0.12	113±11	0.14	115±10	0.15